Widening the directivity patterns of ultrasound transducers using 3-D-printed baffles

Reference:

Kerstens Robin, Laurijssen Dennis, Daems Walter, Steckel Jan.- Widening the directivity patterns of ultrasound transducers using 3-D-printed baffles

IEEE sensors journal / Institute of Electrical and Electronics Engineers [New York, N.Y.] - ISSN 1530-437X - 17:5(2017), p. 1454-1462

Full text (Publishers DOI): http://dx.doi.org/doi:10.1109/JSEN.2016.2642303

Widening the Directivity Patterns of Ultrasound Transducers using 3D-printed Baffles

Robin Kerstens
University of Antwerp
Faculty of Applied Engineering - Electronics-ICT
Antwerp, Belgium
robin.kerstens@uantwerpen.be

Dennis Laurijssen, Walter Daems, Jan Steckel
University of Antwerp
Faculty of Applied Engineering - CoSys-Lab / CZT
Groenenborgerlaan 171, Antwerpen
jan.steckel@uantwerpen.be

***Abstract*—Modern localization and/or mapping systems based on ultrasound use multiple types of ultrasound transducers. These transducers are used to scan the environment and create situational awareness so that obstacles are spotted and collisions may be prevented. Most commercially available transducers however have a Field of View (FOV) that is too limited for these applications. As a result of this, multiple transducers are necessary to get a decent perceptional coverage of the environment. The signals coming from the different transducers can cause unnecessary complications. In this paper we propose a method for widening the FOV of off-the-shelf ultrasonic transducers by creating a baffle that fits on these transducers. This will significantly improve the process of mapping the environment for a wide range of applications such as obstacle avoidance and SLAM. We provide strong experimental evidence for the widening of the directivity patterns by means of various 3D-printed baffles.**

***Index Terms*—Ultrasonic Transducers, Directivity Patterns, In-Air Sonar Systems, 3D prototyping**

I. Introduction

Active in-air sonar sensors gather information from the environment by emitting an ultrasonic pulse through one or more emitters and receiving the reflected echoes with one or more microphones. The field of view (FoV) of the sonar system (i.e., the conical opening angle directed at the section of the environment where information on the environment is gathered) depends directly on the directivity patterns of the emitter and the receiver subsystems. If a sonar sensor with a large field of view is desired, both microphones and transducers of those systems should exhibit a quasi omnidirectional directivity pattern. While small microphones with an omnidirectional directivity pattern exist and are readily available on the market (e.g. MEMS microphones such as the Knowles Acoustics SPU0410HR5H microphone [1]), ultrasonic transducers often have large apertures (required by the desired acoustic output), and therefore narrow directivity patterns (i.e. the acoustic energy is focused in a narrow conical section of the environment) [2]. The need for a large aperture is caused by the fact that a large amount of acoustic energy is needed for sonar operation as the absorption of the ultrasonic signals by the air is quite large [2], [3].

In various sonar systems described in literature [4] [5] [6] [7] the Senscomp 7000 series transducer [8] is readily used (often referred to as the 'Polaroid Transducer' [9]). The directivity patterns of this piston-like transducer can be analytically calculated using a first order Bessel Function [2], which can be seen in Fig. 1 for frequencies ranging from 20 kHz to 80 kHz. Only a horizontal slice of the directivity pattern is shown (elevation = 0°), but it should be noted that the directivity pattern is circular symmetric as the transducer has a circular shape. The acoustic output is focused towards the frontal directions due to the relatively large size of the transducer in comparison to the acoustic wavelengths, limiting the field of view of sonar systems that use this transducer. The directivity pattern of the transducer can be calculated by means of a first order Bessel function. Panel B shows the acoustic output energy (from 20 kHz to 80 kHz) for piston transducers of varying diameters (27mm, 15mm and 10mm). The acoustic energy is focused towards the frontal directions for a transducer with a diameter of 27mm, and is spread more uniformly towards the peripheral angles as the transducer diameter decreases. In previous work the Senscomp 7000 series transducers have been used extensively [7], [10], [11], but the directivity pattern of the Senscomp transducer was found to be limiting in certain applications such as corridor following and obstacle avoidance on a mobile robot. While a small amount of acoustic energy is transmitted to the peripheral angles through diffraction effects [2] around the edge of the transducer mount (see [7]), a more uniform distribution of the acoustic energy would be preferable.

To overcome the limitation of the directivity patterns we therefore propose to reduce the aperture of the transducer by mounting them in a variety of different shapes. By spreading the acoustic energy more omnidirectionally the signal to noise ratio will be lowered in some directions, possibly limiting the achievable range of the sensor. Directions which were previously in the main lobe of the transducer will receive less acoustic energy, as the total amount of energy emitted by the transducer cannot increase with respect to the unbaffled case. The baffle shapes can only introduce a spatial redistribution of the energy. Furthermore, it is possible that the baffle absorbs a certain amount of acoustic energy, which should be reduced as much as possible. The design of the baffle should reduce the abortionist as much as possible, and result in a more uniform distribution of acoustic energy which is favorable for a wide range of applications of ultrasonic sonar sensors. A

wide field of view is for example favorable in applications such as corridor following, as only echoes close to the normal direction of the corridor walls will produce detectable echoes [10]. A similar strategy of adapting the transducer size to the environment can be found in bats who actively modulate their mouth gape to the sensing task at hand [12]. Biologically inspired baffles have been incorporated into man-made sonar sensors to create emitters and receivers with more interesting directivity patterns in [13]–[15]. This biologically inspired method of adding a rigid baffle to a transducer/microphone lies at the base of the approach we propose to follow.

Another way by which the directivity pattern of a transducer can be made more omnidirectional is by using flexible transducer materials, such as EMFIt [16], mounted on non-flat substrates. In [17], the authors use EMFIt on a quasi-spherical surface to achieve near omnidirectional directivity patterns. In [18] we have used a small emitter array (4 channels), constructed using the EMFIt material mounted on a cylindrical surface, to mimic the directivity pattern of the bat P. Discolor. In [19], the authors used EMFIt material on cylindrical and conical surfaces, which also produced very interesting directivity patterns in terms of opening angle. However, the used electromechanical materials suffer from very low acoustic output, which makes them, despite their high acoustic bandwidth, less suitable in long-range sonar applications.

The paper is structured as follows. In section II we will provide an overview of the used hardware and the experimental set up. Section III discusses the used shapes and their selection. Then in section IV there is a discussion of the experimental results. Section V briefly discusses the 3D printing of the baffles and section VI gives an overview of other methods to accomplish transducers with a large FoV. Finally there is a conclusion in section VIII.

II. Hardware overview

To test the effect of adding a baffle, horn or other device on the behavior of the transducer beam pattern we have built several different housings for the Senscomp 7000 transducer. These shapes can be seen in Fig. 3. These were designed using 3D modeling software and constructed using three different 3D printers. Varying the type of printer used allows us to see how much effect the build quality (i.e. the print material used in combination with the layer thickness) will have on the result.

The experimental set-up is shown in Fig. 2. The different shapes tested during this project were all mounted on the transducer using a custom mounting piece. With the microphone array remaining in the same position and the transducer rotating in the horizontal plane ranging from $-90°$ to $90°$ in steps of $1°$, with $0°$ corresponding with the transducer surface facing the microphone, it was possible to generate a directivity pattern for the shape being tested. We only consider the magnitude part of the directivity pattern and do not analyze the phase information of the directivity. This is due to the

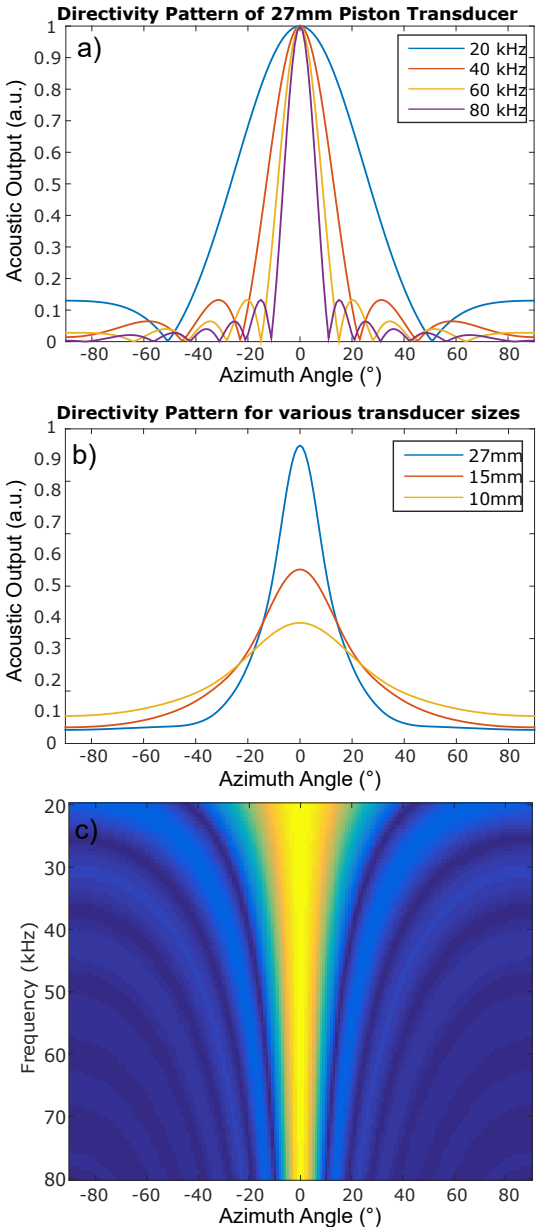

Fig. 1: Panel A: Directivity patterns of a piston transducer with a diameter of 27 mm for frequencies ranging from 20 kHz to 80 kHz in a horizontal slice (elevation of 0°). The acoustic output is focused towards the frontal directions due to the relatively large size of the transducer in comparison to the acoustic wavelengths, possibly limiting the field of view of sonar systems that use this transducer. Panel B shows the acoustic energy (over the band of 20 kHz to 80 kHz.) for piston transducers of varying diameters (27 mm, 15 mm and 10 mm). The acoustic energy is distributed more omnidirectionally with decreasing transducer diameter as expected [2]. Panel C shows the directivity pattern for a 27mm piston-like transducer per frequency, concatenated in a bitmap image. This representation is used throughout the remainder of the paper.

fact that the absolute phase is not of great interest for in-air sonar sensing. Indeed, non-uniformity in the air medium (for example air currents or temperature differences) can have tremendous impact on the absolute phase that is received from a reflector, making phase-based sensing not very robust for the application domain of sonar sensors, ie. in harsh environmental conditions where optic techniques suffer.

The emitted signal is consists of a short hyperbolic frequency sweep going from 80 kHz to 20 kHz in 2ms, windowed using a Hanning window. An in-depth description of the emitted signal can be found in [20]. By collecting azimuth as well as frequency information it is possible to create an image by which we can get a clear view of the capabilities and directivity of the shape being tested. For every azimuthal position of the pan/tilt head 20 spectral measurements were recorded with the three microphones in the array and averaged to increase the signal-to-noise ratio of the resulting data. These generated images are accompanied by a figure of merit. Using this score one can get a quick idea of the acoustical output and the omnidirectionality given by the shape. This will be discussed later.

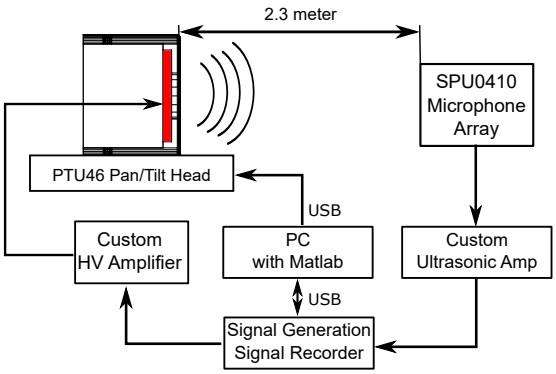

Fig. 2: The experimental set-up

III. Concepts and shapes

It is known from acoustical theory that reducing the size of the aperture will decrease the directivity [2]. To further enhance this effect, several concepts were tried. The primary focus of the shapes designed in this paper is aimed at making them circular symmetric so that the initial circular characteristic of the used transducer is kept, resulting in a circular symmetric directivity pattern. This facilitates the experimental setup for measuring the directivity patterns (the response needs to be measured only in the horizontal plane). An overview of the baffle shapes considered in this paper is depicted in figure 3.

A. Simple Hole Design

This technique will be applied to the Senscomp transducer by creating an enclosure with a hole that has a varying size. The reasoning behind the simple hole design dates back to the early days of science, when Young discussed the behavior of light going through a slit. It was further theorized by Huygens in his work about secondary wavelets [21]. According to Huygens' law, the most omnidirectional result is achieved when the diameter of the aperture is equal to the wavelength being used [21]. Because this paper is aimed at using a linear sweep as an excitation signal (20kHz to 80kHz) instead of a fixed frequency pulse, several hole diameters were used (5 mm, 10 mm and 15 mm) to see which diameter would give the best result for the widest range of frequencies.

B. Inverted Horn Design

The inverted horn design extends the simple hole concept, where a large portion of the transducer would be covered by the overlapping baffle needed to achieve the reduced aperture. By using an inverted horn with an exponential shape it is possible to capture all the generated acoustical output and send the entire bundle through the smaller aperture. Theoretically the result of this shape gives the same directivity pattern as the simple hole design. The only difference would be that the acoustic output level is increased by the amount of energy which would be otherwise trapped beneath the baffle.

C. Filter Design

Combining the simple hole and inverted horn design, this design will get rid of the energy trapped beneath the overlapping baffle needed for the decreased aperture. Inspired by techniques used in high-end speaker systems, an acoustic transmission line is created [22]. The purpose of this transmission line is to divert as much of the unwanted reflection as possible and send it to a region of non-interest. The omnidirectionality and output are caused by the same principles used in the simple hole design, only here, the waves trapped underneath the baffle are not able to interfere with the emitted signal. The absence of this interference should lead to an increase in both omnidirectionality and acoustical output on the one hand, and spectral flatness of the output signal on the other hand.

The design of acoustic filters is discussed in [22]. For this design a first order low-pass filter with a critical frequency of 5 kHz is used. The properties of the filter chamber can be calculated using formula (1):

$$F_c = \frac{s \times c}{\pi \times L(s_1 - s)} \tag{1}$$

Where F_c is cut-off frequency, s is the initial diameter, s_1 is filter chamber diameter, L is the length of the filter chamber and c equals $343\,\mathrm{m\,s^{-1}}$.

It was designed so that it would fit inside the cylindrical hull of the transducer baffle and that the low-frequency signal outlet is located on the side of the shape, just beneath the top layer. Releasing the low frequency signal at the side of the shape should limit the interference with the main signal.

D. Acoustic Lens Technology Design

Acoustic Lens Technology (ALT) is an invention by Sausalito Audio [23] in cooperation with Bang & Olufsen. Initially developed for their Beolab5 speakers [24], this design spreads

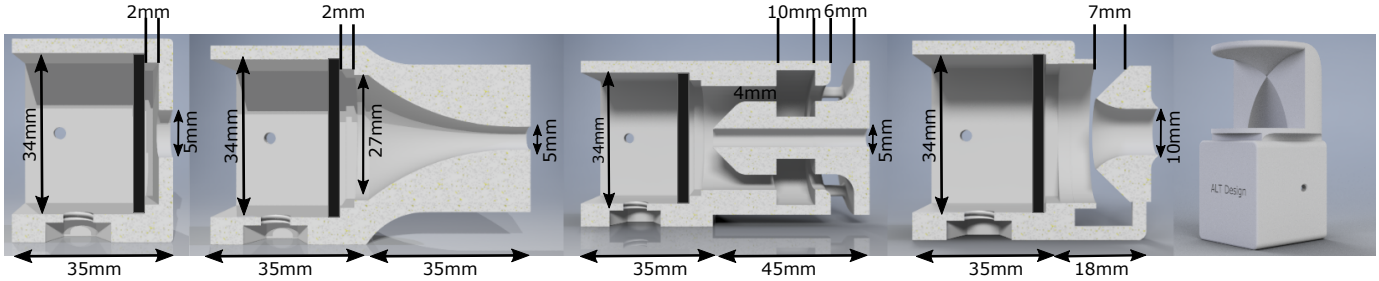

Fig. 3: The five different kinds of shapes used in this paper. From left to right: The simple hole design, inverted horn design, the filter design, the side-gap design and the Acoustic Lens Technology (ALT) design. Variations of each shape shown have been used, altering the aperture of the design. Each shape also features a fixation hole at the bottom to secure it to the pan/tilt head. The rightmost shape also features this hole, but due to its non-symmetrical design it is portrayed from a different angle. The position of the transducer is indicated by the black rectangle. The 3D design files are available upon request through the authors.

the acoustic energy in the room over a surface of 180° [25] [26]. It features a point-to-arc generator, as described in [27]. The design is comparable to the work in [28], but here the cone is altered and the signal is spread out across $180°$ instead of $360°$. Since this design is manufactured for musical purposes the frequency response is expected to be flat [23]. When doing our research we did not find any mention of ALT being used in conjunction with ultrasonic signals. Therefore these two will be combined to see if ALT can be used in our case. The downside of this design is that, due to the lack of circular symmetry in the design the acoustical output is sent only into one plane [27]. While this may be optimal for audio purposes, it is not a desirable feature for sensors to be used with ultrasonic obstacle avoidance or Simultaneous Localization and Mapping (SLAM) applications. Therefore a few adjustments have been made, discussed in the next section. For other applications like corridor following, that rely less on the elevation plane, this design could also serve its purpose.

E. Side-gap Design

The side gap builds upon the filter and the ALT design. The downside of the Filter Design is that a large part of the produced acoustical output is dumped in a useless fashion by diverting reflections into side-regions, which makes the transducer less efficient. By deflecting parts of the signal to the side of the horn there should be a considerable increase in omnidirectionality in the perpendicular plane and acoustical output [28] at and beyond the azimuthal $90°$ position. This design is based on [28] with the addition of the aperture at the center of the cone. The combination of the cone and added aperture should result in an smooth energy distribution in both the horizontal and vertical plane, eliminating the problem of the ALT design.

IV. Experimental validation of proposed baffle shapes

In this section we will provide an experimental methodology for the validation of the proposed baffle shapes. The experimental set-up is shown in Fig. 2, and details on the experimental setup are provided in section II.

A. Data representation and proposed quality metric

The recorded acoustic data is processed using spectral analysis so that the emitted spectrum between 20 kHz and 80 kHz for a specific azimuth angle are shown. Each azimuth value is averaged from 20 measurements with three identical microphones. By taking the average from these microphones a basic form of beam forming is accomplished, focusing the FOV of the microphones in the direction of the transducer. When a recording is made, the received signal is cut off after a specific number of samples in order to decrease multipath reflections coming from the walls next to the experimental set-up. The appropriate number of samples can be calculated using the Time of Flight (ToF) of the direct signal.
The recorded frequency sweep then consists of a signal with a different time value for every frequency in that sweep. This signal is processed using a matched filter, followed by a short-time Fourier transform (STFT, window length = 512, Fs = 360kHz). The position of the pulse from the direct acoustical path is found in the energy content of the STFT. The spectrum on this time position is extracted from the spectrogram for every azimuth angle. This results in a matrix $D(\varphi, f)$ where every column consists out of the estimated spectrum, containing the frequency response of the transducer for that azimuthal value.

We propose to use a quality grading metric to assign a value to the omnidirectionality and the acoustical efficiency given for the whole beam-pattern. The figure of merit for omnidirectionality (G_O) is calculated using the following formula from the recorded directivity pattern $D(\varphi, f)$:

$$D_\varphi = \frac{1}{N_f} \sum_{i=1}^{N_f} P(f_i, \varphi) \tag{2}$$

$$\tilde{D} = \frac{1}{N_\varphi} \sum_{i=1}^{N_\varphi} D_{\varphi_i} \tag{3}$$

$$A_1 = \sum_{i=1}^{N_\varphi} \left| \tilde{D} - D_{\varphi_i} \right| \qquad A_2 = \sum_{i=1}^{N_\varphi} \left| D'_{\varphi_i} \right| \quad (4)$$

$$G_O = \frac{\alpha}{w_1 \cdot A_1 - w_2 \cdot A_2} \qquad \begin{cases} \alpha = 10 \\ w_1 = 1 \\ w_2 = 2 \end{cases} \quad (5)$$

Where G_O is an arbitrary unit representing the Grading for Omnidirectionality. In A_1 (eq. 4) the averages of all φ values (D_φ) are subtracted from the global mean ($\tilde{D}$) to determine how much our beam pattern deviates from a straight line (the optimal case). The second part, A_2 (eq. 4), is the sum of derivatives for each point in the average measurements vector (D_φ), yielding a number that quantifies the curviness of the beam pattern. Because the "curviness" value is small compared to the value of deviation, it is multiplied by weighting factor w_2. α is a value used to make G_O larger, because otherwise it would be very small value. The grading for the acoustical output is an arbitrary unit equal to the mean of all averages of each azimuth value (M). A letter is assigned for each tenth value, so A = 0 to 0.09, B = 0.1 to 0.19, C = 0.2 to 0.29, ... These two values are combined into the MG_O score (e.g. C2.3456 has a mean output value (M) between 0.2 and 0.29, and a G_O of 2.3456.). It should be noted that the scoring system is not linear, and should only be interpreted as the higher scores achieving a better result than the lower scores.

B. Results

During the first measurements it quickly became clear that the frequency response of the used Knowles SPU0410 microphone is not flat beyond the 10 kHz barrier, causing serious sensitivity spikes around 20 kHz and 50 kHz. To counter this effect a custom transducer has been made from the EMFIt material, which has a very linear frequency response op to 250 kHz [16], [29], [30]. Taking the average from several measurements, the directivity pattern and spectral content of the recorded signal from the EMFI transducer was calculated. Due to the known flat emission spectrum of the EMFIt material we can assume that any deviation from a flat spectrum is caused by the frequency response of the microphones (see Fig. 4). This measurement of the microphones' transfer function was then used to compensate the subsequent results using the senscomp transducers and the baffles. In these results a peak around 50 kHz remains because this is also the resonance frequency of the Senscomp 7000 [8]. The remaining frequency-amplitude-error is believed to be of lesser importance since the main goal of this paper is the design of shapes for a larger FOV, with less of an emphasis on the specific frequency-output.

1) Simple Hole Design: In Fig. 5 there is a visualization of the effect of narrowing the aperture on the beam pattern. The smaller aperture of 5 mm delivers a emission pattern in which the acoustic energy is more evenly spread across all angles and frequencies. The best results is achieved when an aperture of 5 mm is used (a wavelength of 5 mm is equal to 68.6 kHz; $f = 343/(5 \cdot 10^{-3})$). Around 32 kHz there is even an almost

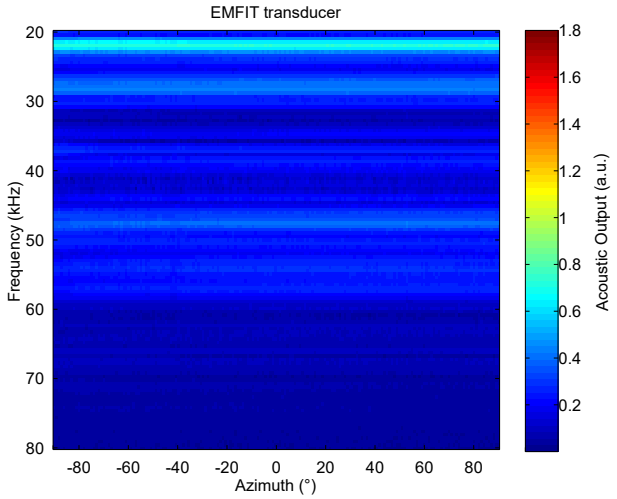

Fig. 4: Beam pattern $D(\varphi, f)$ for the circular EMFIT transducer, with a clearly omnidirectional pattern.

omnidirectional band. An explanation for this effect is in the characteristics of the Senscomp 7000 transducer itself, which has a resonant point around 50 kHz. This in combination with an aperture diameter suited for a wavelength close to that of the resonant frequency explains the positive result at this point. As expected from a theoretical point of view, as the aperture of the baffle gets smaller, the acoustic energy is more smeared out spatially. Making the aperture larger would increase the output, but also increase the directivity, which might be an unwanted effect.

2) Inverted Horn Design: To counter standing wave losses within the baffles caused by the overlapping material needed for the decreased aperture, an inverted horn is introduced. The measurement results in Fig. 6 show that this approach has a positive effect on the mean acoustical output, which has increased compared to the simple hole designs in Fig. 5. An unexpected effect is the slight increase of directivity in the result, which was expected to remain equal to that of the simple hole designs. There is also an introduction of spectral notches, which are caused by some remaining standing waves originating from the horn shape. The results in Fig. 6 show that these notches are present in all inverted horn designs.

3) Filter Design: Assuming the spectral notches found in the inverted horn designs are caused by internal reflections, a method was developed that would cancel out these reflections. The filter design in Fig. 7 shows that these frequency dependent notches are indeed gone. The combination of the simple hole design (Fig. 5) and the added filter results in an improved acoustical output and omnidirectionality. Given an MG_O of C3.6293 this shape has the highest score (for two-plane omnidirectionality), which could be improved even more with some slight adjustments in the construction of the shape of the baffle and acoustic filter. The divergence of the beam pattern from a flat beam pattern are believed to be caused by

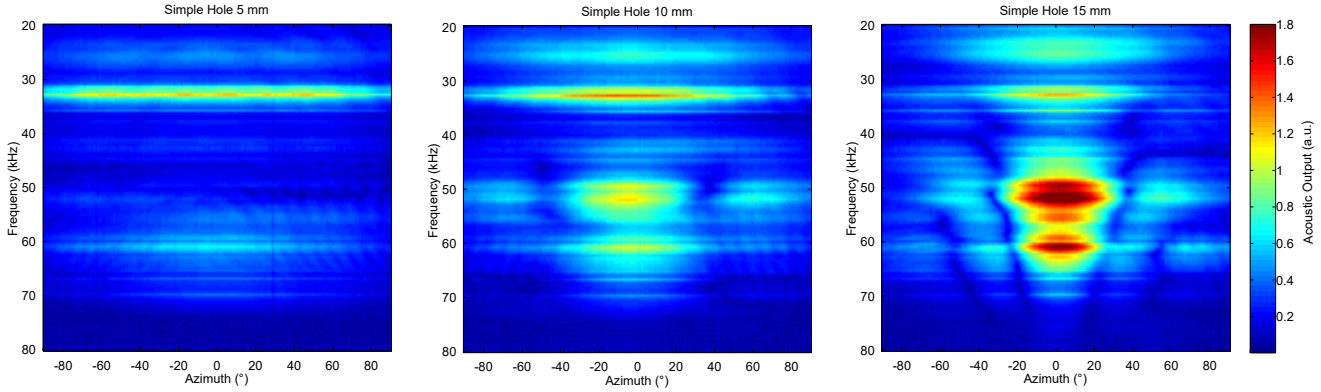

Fig. 5: Beam pattern $D(\varphi, f)$ for the Simple Hole Designs with an aperture of 5 mm and an MG_O score of C2.0608 (left), an aperture of 10 mm and an MG_O score of D0.68043 (center) and an aperture of 15 mm and an MG_O score of D0.41548 (right). The acoustic output is distributed evenly over all angles, but the mean acoustic output has somewhat decreased due to standing wave losses in the baffle enclosure. This loss of acoustic energy can be overcome by using an inverted horn-shaped baffle.

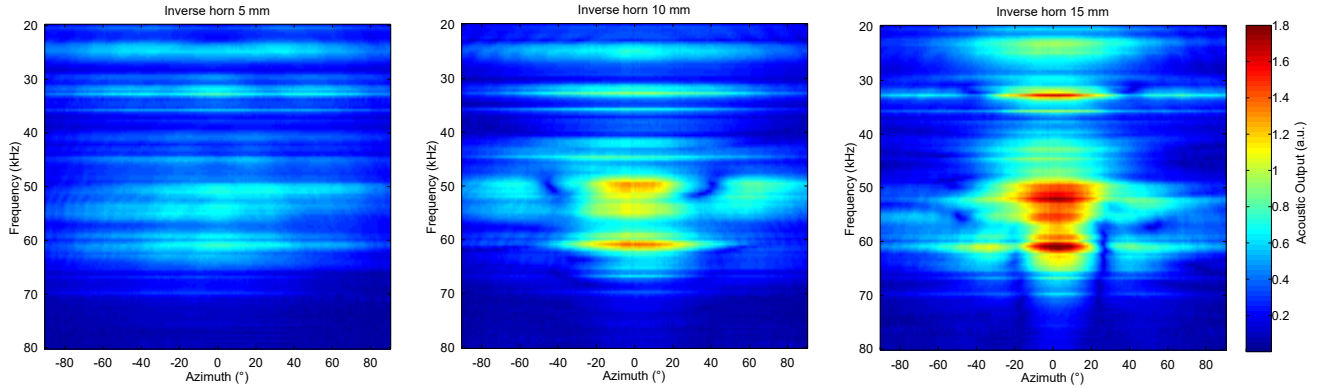

Fig. 6: Beam pattern $D(\varphi, f)$ for the Inverted Horn Design with an aperture of 5 mm and an MG_O score of D1.2904 (left), an aperture of 10 mm and an MG_O score of D0.64739 (center), an aperture of 15 mm and an MG_O score of E0.38526 (right). The acoustic output is distributed more evenly and the mean acoustic output has increased compared to the simple hole design. Spectral notches are present in the acoustic output, which is caused by the interaction of the acoustic waves with the shape of the inverted horn.

the shape of the baffle: the low-frequency signal, released at the side of the shape (see Fig. 3) will refract around the edges and distort the high-frequency signal coming from the center aperture. When the aperture increases, the similarities with the non-filtered counterpart become more apparent (see Fig. 7 vs. Fig. 5). Again, notice the increase in acoustical output because of the added filter.

4) Side-Gap Design: Building on the principles used in the ALT design, trying to further enhance the omnidirectionality of the directivity pattern, the cone was extended to cover a field of $360°$ and an extra aperture was added in the center of the floating cone (the shape also becomes circular symmetric because of this). Using these features the signal can be emitted into omnidirectionally instead of only in the horizontal plane. The first panel of Fig. 8 shows the vertical plane of the directivity pattern. Again, because of the same refraction found in the filter design, some angle-dependent spectral notches are found. With an MG_O of E0.6165, and some measurements even going to an MG_O of F0.5372, this shape gives the highest acoustical output of all when the transducer is in the vertical position. A surprising result is that if the transducer is in the horizontal position the level of acoustical output is close to the same as in the vertical position, only now the G_O score is close to omnidirectional. Also when the transducer is tilted $45°$ a slightly more silent region (C instead of D) is found, but also with a directivity pattern that is certainly usable for tracking applications.

5) ALT Design: Another approach to cancel the directivity and frequency related problems is the ALT Design. Fig. 9 shows clear improvement in loss of directivity and shows no signs of frequency-dependence. As shown here, the design is not only suitable for audible frequencies, but also for

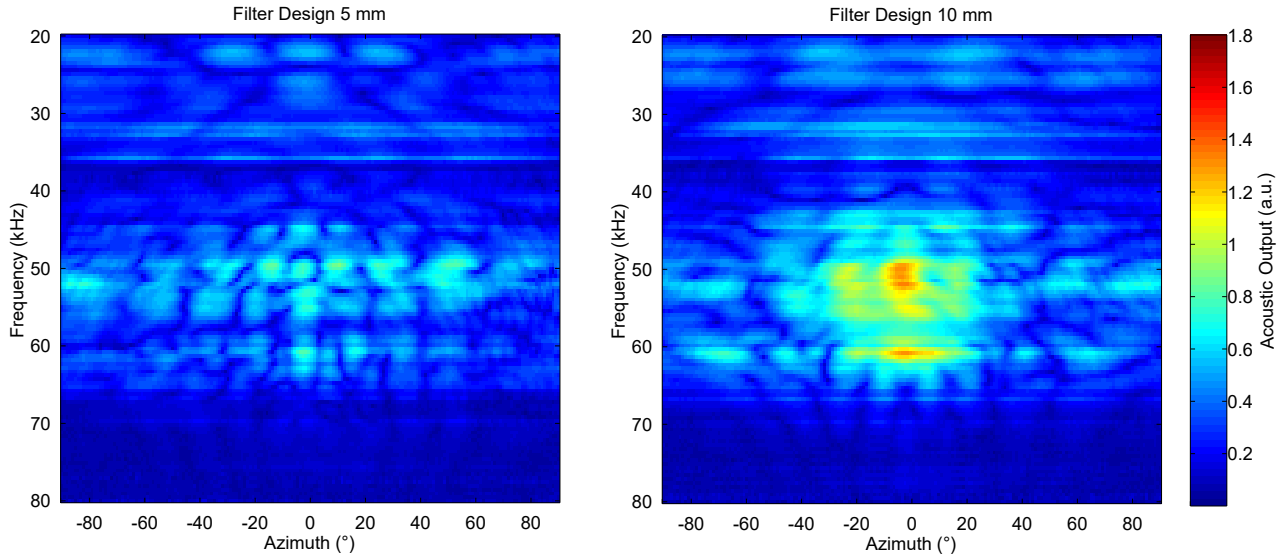

Fig. 7: Beam pattern $D(\varphi, f)$ for the Filter Design with an aperture of 5 mm and an MG_O score of C3.6293 (left) and an aperture of 10 mm and an MG_O score of D0.79703 (right).

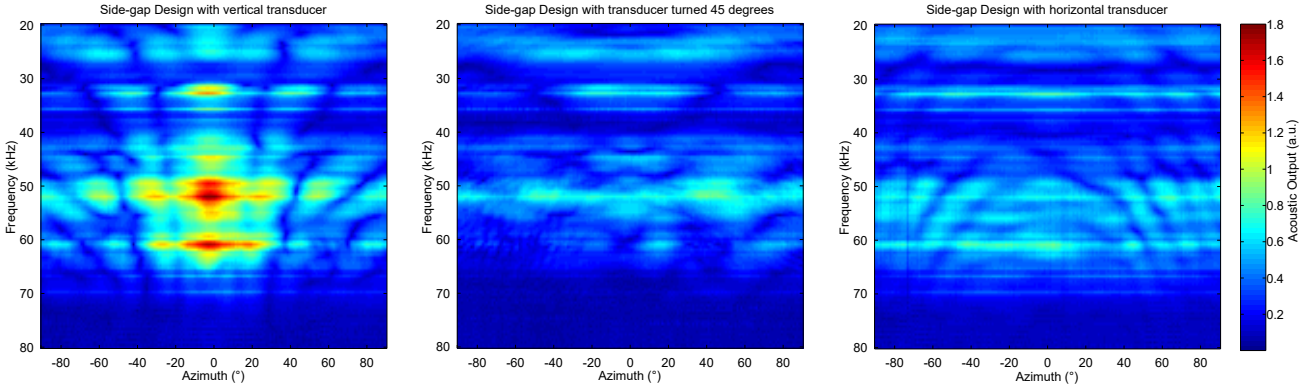

Fig. 8: Beam pattern $D(\varphi, f)$ for the Side-Gap Design with an aperture of 10 mm in different positions. First with the transducer in vertical position and MG_O score of E0.61653 (left), tilted 45°the MG_O score is C2.9754 (center) and when the transducer is in horizontal position (right), it becomes omnidirectional with an MG_O score of D20.0426.

ultrasonic frequencies. Note that this design does not produce a circular symmetric directivity pattern, but only provides omnidirectional signal emission in the horizontal plane.

V. 3D PRINTING FOR CONSTRUCTION

One of the main topics of this research is of course the construction of the shapes used. The fast-growing popularity of 3D-print prototyping offers a lot of possibilities, and with the many different options available today one might wonder if these differences in machinery and material play an important role when prototyping a device to be used with ultrasonic signals. Due to the small wavelengths of ultrasound this is certainly to be expected. In order to research this topic three different 3D printers and printing materials have been used. Table I gives an overview of these printers, along with some extra info such as print material and pricing. Please do note that the UP Mini was slightly modified by the owner to achieve better printer results. The modifications include upgraded nozzle heating and bottom plate. The cost of these modifications is not included in Table I because it is small compared to the cost of the printer itself.

	UP Mini	Makerbot Replicator	Stratasys Object Eden 260V
Printmaterial	ABS	PLA	Vero Blue
Layer Thickness	0.2 mm	0.25 mm	0.02 mm
Printer Cost	∼600 euro	∼2560 euro	∼17500 euro
Cost per shape	∼0.75 euro	∼1.65 euro	∼15-30 euro

TABLE I: 3D Printer overview

To test the influence of the different 3D-printers and material an ANOVA method was chosen to calculate the significance.

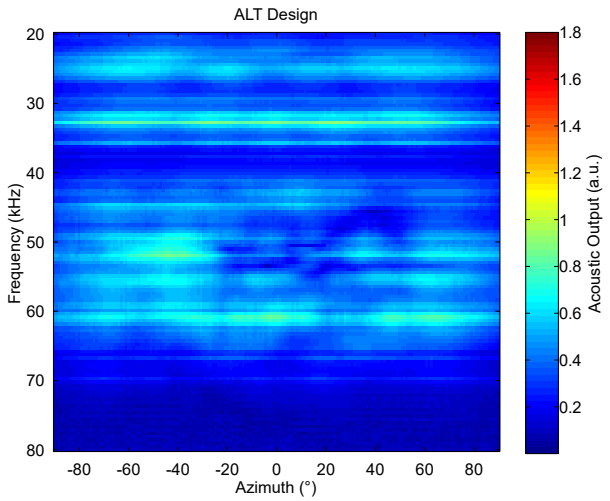

Fig. 9: Beam pattern $D(\varphi, f)$ for the ALT Design, given an MG_O score of D3.9475. The directivity pattern of this baffle shape shows exceptional spectral and angular flatness, showing that the ALT principle can be transferred from audible to ultrasonic frequencies. Note that this design does not produce a circular symmetric directivity pattern, but only provides omnidirectional signal emission in the horizontal plane, which makes it less suited for the intended applications.

Again, to minimize extraneous factors, a completely randomized design and measurement sequence was used. Using the shape of the inverted horn with an aperture diameter of 15 mm as test, three copies were made. As shown in Fig. 11 and Table I there are slight differences in quality.

The box-plot result of the ANOVA can be seen in Fig. 10. Here a surprising result occurs in which the shape printed by the Makerbot Replicator (using PLA material) receives a higher score for nearly all measurements. The result of the ANOVA-test is used to confirm these results. The test resulted in a P-value of 0.036. This is smaller than the significance level (α) of 0.05 and means that the null hypothesis can be rejected [31] and the alternative hypothesis can not, which means that there is indeed a statistical significant influence of the printer and it's printing material used on the G_O.

A possible explanation for this effect can be the fact that the shape made with the Makerbot Replicator has the thickest layers, see Table I. Although the difference is only 0.05 mm compared to the UP Mini, the effect has been observed and should not be ignored. The rougher surface of the resulting baffle might cause additional diffraction, which result in a more omnidirectional directivity pattern. This might positively impact the applicability of baffle shapes in low-cost sonar sensors, since the prototypes made with the Makerbot cost significantly less than those made with the high-end Stratasys printer.

VI. Conclusion and Future Work

The work in this paper started from the fact that current high acoustic output transducer often have a very narrow

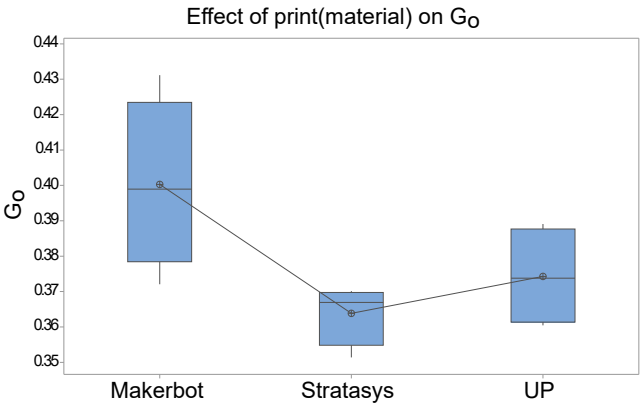

Fig. 10: Comparison of the effect on printer(material) on G_O with an inverse horn with an aperture of 15 mm.

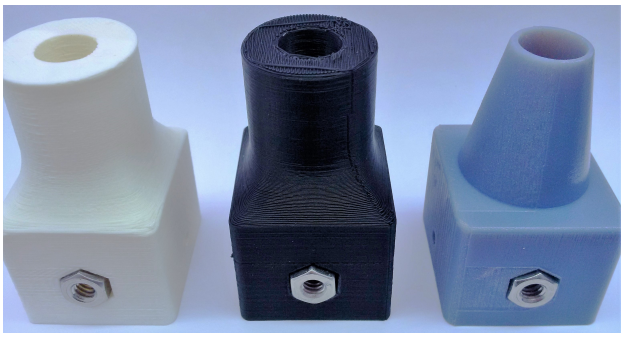

Fig. 11: The inverted horn shape obtained by printing the same design file using three different printers. White: UP Mini, Black: Makerbot Replicator, Blue: Stratasys Eden v260 (slightly adjusted to save printing material). Due to the higher layer thickness, the shape produced by the Makerbot exhibits more surface roughness, which introduces more diffractions, causing the directivity patterns from this shape to be more omnidirectional.

directivity pattern. From this, we recognized the need for widening the field of view in many sonar-sensor applications, without significantly reducing the overall emitted acoustic energy (i.e. only redistributing the acoustic energy is allowed). This problem was solved by adding customized baffles to the widely used Senscomp 7000-series ultrasonic transducer. These baffles were all experimentally validated and successfully enlarge the Field of View of the transducer to the point of near-omnidirectionality. Several shapes were designed that succeed in this, or at least succeed in one plane. The latter can still be used in applications where only one plane is the most important such as corridor following using acoustic flow [32]. Another surprising conclusion is the fact that the manufacturing technique used for the baffles has a significant role, as the small difference in layer thickness from the baffles printed with the cheaper printers will add to the diffraction of the baffle and help decrease the directivity of the acoustic

output.

Work based on this paper could further explore the possibilities of both the filter design and the side-gap design. Experimenting with series filters or more complex filter-chambers is certainly interesting. The same is valid for the side-gap design, where one might investigate a way to reduce the difference between the horizontal and vertical beam pattern so it becomes a more consistent whole.

REFERENCES

[1] Knowels Acoustics, *"Knowles Acoustics"*, Std. [Online]. Available: http://www.knowles.com

[2] A. D. Pierce, *Acoustics: An Introduction to Its Physical Principles and Applications*. Springer Science+Business Media, 1990.

[3] J. A. Thomas, and C. F. Moss, and M. Vater, "Echolocation in bats and dolphins," 2004.

[4] H. Peremans, and K. Audenaert, and J. Van Campenhout, "A high-resolution sensor based on tri-aural perception,," *IEEE Transactions on Robotics and Automation*, vol. 9, no. 1, pp. 36–48, 1993. [Online]. Available: http://ieeexplore.ieee.org/lpdocs/epic03/wrapper.htm?arnumber=210793

[5] J. Reijniers and H. Peremans, "Biomimetic sonar system performing spectrum-based localization,," *Robotics, IEEE Transactions on*, vol. 23, no. 6, pp. 1151–1159, 2007. [Online]. Available: http://ieeexplore.ieee.org/xpls/abs_all.jsp?arnumber=4359264

[6] R. Kuc, "Generating b-scans of the environment with a conventional sonar,," *Sensors Journal, IEEE,*, vol. 8, no. 2, pp. 151–160, 2008. [Online]. Available: http://ieeexplore.ieee.org/xpls/abs_all.jsp?arnumber=4427204

[7] J. Steckel, and A. Boen and H. Peremans, "Broadband 3-D sonar system using a sparse array for indoor navigation,," *IEEE Transactions on Robotics*, vol. 29, no. 1, pp. 161–171, 2013. [Online]. Available: http://ieeexplore.ieee.org/lpdocs/epic03/wrapper.htm?arnumber=6331017

[8] SensComp, *SensComp 7000 datasheet*, SensComp, 2008.

[9] C. Biber, and S. Ellin, and E. Shenk, and J. Stempeck, "The polaroid ultrasonic ranging system," *Audio Engineering Society Convention 67*, 1980. [Online]. Available: http://www.aes.org/e-lib/browse.cfm?elib=3680

[10] H. Peremans and J. Steckel, "Acoustic flow for robot motion control,," *2014 IEEE International Conference Robotics and Automation (ICRA)*, 2014.

[11] J. Steckel, "Sonar system combining an emitter array with a sparse receiver array for air-coupled applications," *IEEE Sensors Journal*, vol. PP, no. 99, pp. 1–1, 2015. [Online]. Available: http://ieeexplore.ieee.org/lpdocs/epic03/wrapper.htm?arnumber=7008433

[12] P. Kounitsky, and J. Rydell, and E. Amichai, and A. Boonman, and O. Eitan, and A. J. Weiss, and Y. Yovel, "Bats adjust their mouth gape to zoom their biosonar field of view," *Proceedings of the National Academy of Sciences of the United States of America*, vol. 112, no. 21, 2015. [Online]. Available: http://www.pnas.org/content/112/21/6724.short

[13] F. Schillebeeckx, F. De Mey, D. Vanderelst, and H. Peremans, "Biomimetic sonar: Binaural 3d localization using artificial bat pinnae," *The International Journal of Robotics Research*, p. 0278364910380474, 2010.

[14] Y. Fu, P. Caspers, and R. Müller, "A dynamic ultrasonic emitter inspired by horseshoe bat noseleaves," *Bioinspiration & biomimetics*, vol. 11, no. 3, p. 036007, 2016.

[15] F. Guarato, H. Andrews, J. F. Windmill, J. Jackson, G. Pierce, and A. Gachagan, "Features in geometric receiver shapes modelling bat-like directivity patterns," *Bioinspiration & biomimetics*, vol. 10, no. 5, p. 056007, 2015.

[16] S. Rupitsch, R. Lerch, J. Strobel, and A. Streicher, "Ultrasound transducers based on ferroelectret materials," *IEEE Transactions on Dielectrics and Electrical Insulation*, vol. 18, no. 1, pp. 69–80, feb 2011. [Online]. Available: http://ieeexplore.ieee.org/document/5704495/

[17] J. L. Ealo, F. Seco, C. Prieto, A. R. Jimenez, J. Roa, A. Koutsou, and J. Guevara, "Customizable field airborne ultrasonic transducers based on electromechanical film," in *2008 IEEE Ultrasonics Symposium*. IEEE, nov 2008, pp. 879–882. [Online]. Available: http://ieeexplore.ieee.org/document/4803657/

[18] J. Steckel and H. Peremans, "A novel biomimetic sonarhead using beamforming technology to mimic bat echolocation," *IEEE Transactions on Ultrasonics, Ferroelectrics, and Frequency Control*, vol. 59, pp. 1369–1377, 2012.

[19] J. Ealo, F. Seco, and A. Jimenez, "Broadband EMFi-based transducers for ultrasonic air applications," *IEEE Transactions on Ultrasonics, Ferroelectrics and Frequency Control*, vol. 55, no. 4, pp. 919–929, apr 2008. [Online]. Available: http://ieeexplore.ieee.org/document/4494787/

[20] J. Steckel, A. Boen, and H. Peremans, "Broadband 3-d sonar system using a sparse array for indoor navigation," *IEEE Transactions on Robotics*, vol. 29, no. 1, pp. 161–171, 2013.

[21] C. Huyghens, *Traité de la lumière*. Gauthier-Villars, 1690.

[22] D. R. Raichel, *The science and applications of acoustics*. Springer Science+Business Media, 2006.

[23] D. Moulton, "The use of an acoustic lens to control the high frequency dispersion of conventional soft dome radiators," American Loudspeaker Manufacturers Association Symposium, Las Vegas, NV, Tech. Rep., Jan. 1998.

[24] David Moulton, and Poul Praestgaard, and Jan A. Pedersen, "A new loudspeaker design: a case study of an effort to more fully integrate the loudspeaker into the playback room in a musical way," May 2003.

[25] E. LaCarrubba, "Apparatus for the redistribution of acoustic energy," Patent, May, 2000, uS Patent 6,068,080. [Online]. Available: https://www.google.com/patents/US6068080

[26] P. Chapman and M. Olsen, "An apparatus for redistributing acoustic energy," Patent, Apr., 2015, wO Patent App. PCT/EP2014/072,211. [Online]. Available: https://www.google.com/patents/WO2015055763A1?cl=en

[27] Paul K. Manhart, K. Scott Ellis, "SWept conics: Single mirror transformers," 2015.

[28] R. W. Claycomb, "Omni-directional ultrasonic transducer for robotic navigation," 1992.

[29] Joao L. Ealo, and Fernando Seco, and Antonia R. Jimenez, "Broadband emfi-based transducers for ultrasonic air applications," *IEEE Transactions on Ultrasonics, Ferroelectrics, and Frequency Control*, vol. 55, no. 4, 2008.

[30] A. Streicher, and M. Kaltenbacher, and R. Lerch, and H. Peremans, "Broadband emfi ultrasonic transducer for bat research," 2006.

[31] Montgomery, Douglas C, *Design and Analysis of Experiments*, 2nd ed. Wiley, 1984.

[32] Peremans, Herbert and Steckel, Jan, "Acoustic Flow for Robot Motion Control," in *Robotics and Automation (ICRA), 2014 IEEE International Conference on*, 2014.

[33] B. . Olufsen, "Beolab 5." [Online]. Available: http://www.bang-olufsen.com/en/sound/loudspeakers/beolab-5

[34] M. J. Anderson and P. J. Whitcomb, *DOE simplified*. Productivity, 2000.

[35] E. Ltd, *"EMFIT"*, Std. [Online]. Available: https://www.emfit.com/electroactive-polymers

[36] D. P. Massa, *An Overview of Electroacoustic Transducers*. Massa Products Corporation, 2015.

[37] A. Day, Robert, "PVdf and array transducers," 1996. [Online]. Available: http://www.ndt.net/article/rocky/rocky.htm

[38] M. Gaal, J. Bartusch, E. Dohse, F. Schadow, and E. Köppe, "Focusing of ferroelectret air-coupled ultrasound transducers," vol. 1706. AIP Publishing, 2016, p. 080001. [Online]. Available: http://scitation.aip.org/content/aip/proceeding/aipcp/10.1063/1.4940533